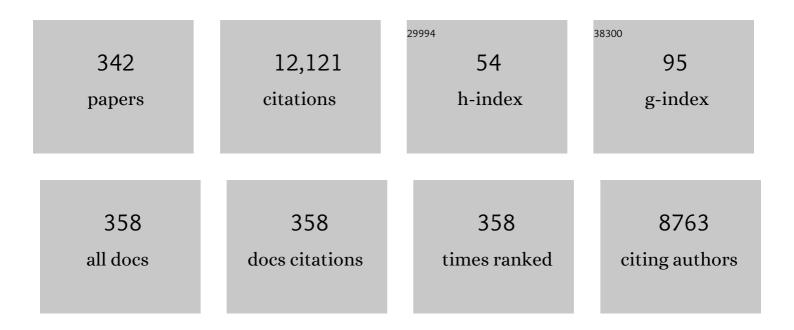
List of Publications by Year in descending order

Source: https://exaly.com/author-pdf/3038522/publications.pdf Version: 2024-02-01



FLINS VILLEC

#	Article	IF	CITATIONS
1	Combining Viedma Ripening and Temperature Cycling Deracemization. Crystal Growth and Design, 2022, 22, 1874-1881.	1.4	10
2	Influence of Ostwald's Rule of Stages in the Deracemization of a Compound Using a Racemic Resolving Agent. Crystal Growth and Design, 2022, 22, 1459-1466.	1.4	1
3	Ultrathin GaAs solar cells with a high surface roughness GaP layer for lightâ€trapping application. Progress in Photovoltaics: Research and Applications, 2022, 30, 622-631.	4.4	10
4	Improvements in ultraâ€light and flexible epitaxial liftâ€off GaInP/GaAs/GaInAs solar cells for space applications. Progress in Photovoltaics: Research and Applications, 2022, 30, 1003-1011.	4.4	17
5	Comprehensive analysis of photon dynamics in thin-film GaAs solar cells with planar and textured rear mirrors. Solar Energy Materials and Solar Cells, 2022, 244, 111708.	3.0	6
6	A study of the hydration and dehydration transitions of SrCl2 hydrates for use in heat storage. Solar Energy Materials and Solar Cells, 2022, 242, 111770.	3.0	14
7	Ordered and Disordered Carboxylic Acid Monolayers on Calcite (104) and Muscovite (001) Surfaces. Journal of Physical Chemistry C, 2022, 126, 8855-8862.	1.5	2
8	Limiting mechanisms for photon recycling in thinâ€film GaAs solar cells. Progress in Photovoltaics: Research and Applications, 2021, 29, 379-390.	4.4	10
9	Cocrystals of Praziquantel: Discovery by Network-Based Link Prediction. Crystal Growth and Design, 2021, 21, 3428-3437.	1.4	24
10	Proton irradiation induced GaAs solar cell performance degradation simulations using a physics-based model. Solar Energy Materials and Solar Cells, 2021, 223, 110971.	3.0	10
11	Dark curve analysis of thin-film GaAs solar cells, with a focus on photon recycling approaches. , 2021, , .		0
12	Combining Diastereomeric Resolution and Viedma Ripening by Using a Racemic Resolving Agent. European Journal of Organic Chemistry, 2021, 2021, 5975.	1.2	4
13	In-situ XRD study on the selenisation parameters driving Ga/In interdiffusion in Cu(In,Ga)Se2 in a versatile, industrially-relevant selenisation furnace. Solar Energy, 2021, 230, 1085-1094.	2.9	4
14	Monovalent – divalent cation competition at the muscovite mica surface: Experiment and theory. Journal of Colloid and Interface Science, 2020, 559, 291-303.	5.0	14
15	Photoracemizationâ€Based Viedma Ripening of a BINOL Derivative. Chemistry - A European Journal, 2020, 26, 839-844.	1.7	29
16	A facile lightâ€trapping approach for ultrathin GaAs solar cells using wet chemical etching. Progress in Photovoltaics: Research and Applications, 2020, 28, 200-209.	4.4	41
17	Organothiol Monolayer Formation Directly on Muscovite Mica. Angewandte Chemie, 2020, 132, 2343-2347.	1.6	1
18	Organothiol Monolayer Formation Directly on Muscovite Mica. Angewandte Chemie - International Edition, 2020, 59, 2323-2327.	7.2	4

#	Article	IF	CITATIONS
19	Calcite (104) Surface–Electrolyte Structure: A 3D Comparison of Surface X-ray Diffraction and Simulations. Journal of Physical Chemistry C, 2020, 124, 18564-18575.	1.5	23
20	Coâ€crystal Prediction by Artificial Neural Networks**. Angewandte Chemie - International Edition, 2020, 59, 21711-21718.	7.2	53
21	Coâ€crystal Prediction by Artificial Neural Networks**. Angewandte Chemie, 2020, 132, 21895-21902.	1.6	7
22	Observation and implications of the Franzâ€Keldysh effect in ultrathin GaAs solar cells. Progress in Photovoltaics: Research and Applications, 2020, 28, 779-787.	4.4	15
23	Epitaxy of Rhodochrosite (MnCO <sub>3</sub> ) on Muscovite Mica and Its Relation with Calcite (CaCO <sub>3</sub> ). Crystal Growth and Design, 2020, 20, 4802-4810.	1.4	2
24	Complex Geometric Structure of a Simple Solid-Liquid Interface: GaN(0001)-Ga. Physical Review Letters, 2020, 124, 086101.	2.9	6
25	Electron radiation–induced degradation of GaAs solar cells with different architectures. Progress in Photovoltaics: Research and Applications, 2020, 28, 266-278.	4.4	19
26	On the mechanism of solid-state phase transitions in molecular crystals – the role of cooperative motion in (quasi)racemic linear amino acids. IUCrJ, 2020, 7, 331-341.	1.0	28
27	Quantum Dot-Based Thin-Film III–V Solar Cells. Lecture Notes in Nanoscale Science and Technology, 2020, , 1-48.	0.4	2
28	Epitaxial Lift-Off of Ultra-Thin GaAs Solar Cells with Textured Back Contact Layer and Diffuse Silver Mirror. , 2020, , .		2
29	Exploring the Franz-Keldysh effect in ultra-thin GaAs solar cells. , 2020, , .		1
30	Deracemization in a Complex Quaternary System with a Secondâ€Order Asymmetric Transformation by Using Phase Diagram Studies. Chemistry - A European Journal, 2019, 25, 13890-13898.	1.7	8
31	Deracemization in a Complex Quaternary System with a Secondâ€Order Asymmetric Transformation by Using Phase Diagram Studies. Chemistry - A European Journal, 2019, 25, 13837-13837.	1.7	2
32	The Crystalline Sponge Method in Water. Chemistry - A European Journal, 2019, 25, 14999-15003.	1.7	27
33	Toward Continuous Deracemization via Racemic Crystal Transformation Monitored by in Situ Raman Spectroscopy. Crystal Growth and Design, 2019, 19, 5858-5868.	1.4	12
34	Epitaxial Crystallization of Insulin on an Ordered 2D Polymer Template. Chemistry - A European Journal, 2019, 25, 3756-3760.	1.7	2
35	Racemization and Deracemization through Intermolecular Redox Behaviour. Chemistry - A European Journal, 2019, 25, 9639-9642.	1.7	5
36	Cocrystals in the Cambridge Structural Database: a network approach. Acta Crystallographica Section B: Structural Science, Crystal Engineering and Materials, 2019, 75, 371-383.	0.5	25

#	Article	IF	CITATIONS
37	Advanced Lightweight Flexible Array with Mechanical Architecture. , 2019, , .		1
38	Wet-Chemically Textured Ultra-Thin GaAs Solar Cells with Dielectric/Metal Rear Mirrors. , 2019, , .		0
39	Cocrystal design by network-based link prediction. CrystEngComm, 2019, 21, 6875-6885.	1.3	32
40	Attritionâ€Enhanced Deracemization of the Antimalaria Drug Mefloquine. Angewandte Chemie, 2019, 131, 1684-1687.	1.6	5
41	Attritionâ€Enhanced Deracemization of the Antimalaria Drug Mefloquine. Angewandte Chemie - International Edition, 2019, 58, 1670-1673.	7.2	26
42	The crystal structures of four dimethoxybenzaldehyde isomers. Acta Crystallographica Section E: Crystallographic Communications, 2019, 75, 38-42.	0.2	1
43	The crystalline sponge method: pitfalls, challenges and solutions. Acta Crystallographica Section A: Foundations and Advances, 2019, 75, e514-e514.	0.0	0
44	Surfaces with Controllable Topography and Chemistry Used as a Template for Protein Crystallization. Crystal Growth and Design, 2018, 18, 763-769.	1.4	5
45	Concentration-Dependent Adsorption of CsI at the Muscovite–Electrolyte Interface. Langmuir, 2018, 34, 3821-3826.	1.6	18
46	Amides as anticaking agents for sodium chloride: is a triple branched variant necessary?. CrystEngComm, 2018, 20, 334-339.	1.3	2
47	Partially shaded III-V concentrator solar cell performance. Solar Energy Materials and Solar Cells, 2018, 179, 231-240.	3.0	7
48	Deracemization of a Racemic Compound by Using Tailorâ€Made Additives. Chemistry - A European Journal, 2018, 24, 2863-2867.	1.7	14
49	Solid–Liquid Interface Structure of Muscovite Mica in SrCl <sub>2</sub> and BaCl <sub>2</sub> Solutions. Langmuir, 2018, 34, 4241-4248.	1.6	12
50	Additive Induced Formation of Ultrathin Sodium Chloride Needle Crystals. Crystal Growth and Design, 2018, 18, 755-762.	1.4	12
51	The Rich Solid-State Phase Behavior of dl-Aminoheptanoic Acid: Five Polymorphic Forms and Their Phase Transitions. Crystal Growth and Design, 2018, 18, 242-252.	1.4	11
52	Racemic and Enantiopure Camphene and Pinene Studied by the Crystalline Sponge Method. Crystal Growth and Design, 2018, 18, 126-132.	1.4	19
53	Increased Performance of Thin-film GaAs Solar Cells with Improved Rear Interface Reflectivity. , 2018, ,		0
54	Solidâ€Phase Conversion of Four Stereoisomers into a Single Enantiomer. Angewandte Chemie, 2018, 130, 15667-15670.	1.6	6

#	Article	IF	CITATIONS
55	Solidâ€Phase Conversion of Four Stereoisomers into a Single Enantiomer. Angewandte Chemie - International Edition, 2018, 57, 15441-15444.	7.2	22
56	Water Structure, Dynamics and Ion Adsorption at the Aqueous {010} Brushite Surface. Minerals (Basel, Switzerland), 2018, 8, 334.	0.8	8
57	Role of Additives during Deracemization Using Temperature Cycling. Crystal Growth and Design, 2018, 18, 6617-6620.	1.4	24
58	Critical vacancy density for melting in two-dimensions: the case of high density Bi on Cu(111). New Journal of Physics, 2018, 20, 083045.	1.2	0
59	Additive induced pseudo-homoepitaxy of nanoneedles on NaCl crystals. Journal of Crystal Growth, 2018, 498, 43-50.	0.7	4
60	Increased performance of thin-film GaAs solar cells by rear contact/mirror patterning. Thin Solid Films, 2018, 660, 10-18.	0.8	30
61	Influence of laterally split spectral illumination on multi-junction CPV solar cell performance. Solar Energy, 2018, 170, 86-94.	2.9	6
62	The structure of PbCl2on the {100} surface of NaCl and its consequences for crystal growth. Journal of Chemical Physics, 2018, 148, 144703.	1.2	1
63	Epitaxy of Anthraquinone on (100) NaCl: A Quantitative Approach. Crystal Growth and Design, 2018, 18, 5099-5107.	1.4	3
64	Discovering new cocrystals via coformer–network analysis. Acta Crystallographica Section A: Foundations and Advances, 2018, 74, e339-e339.	0.0	0
65	The illumination angle dependency of CPV solar cell electrical performance. Solar Energy, 2017, 144, 166-174.	2.9	21
66	Metal diffusion barriers for GaAs solar cells. Physical Chemistry Chemical Physics, 2017, 19, 7607-7616.	1.3	6
67	Observation of Ultrathin Precursor Film Formation during Ge–Si Liquid-Phase Epitaxy from an Undersaturated Solution. Langmuir, 2017, 33, 814-819.	1.6	5
68	Additive Enhanced Creeping of Sodium Chloride Crystals. Crystal Growth and Design, 2017, 17, 3107-3115.	1.4	13
69	Noble metal surface degradation induced by organothiols. Surface Science, 2017, 662, 59-66.	0.8	3
70	Temperature-Induced Degradation of Thin-Film III–V Solar Cells for Space Applications. IEEE Journal of Photovoltaics, 2017, 7, 702-708.	1.5	14
71	Solid Phase Deracemization of an Atropisomer. Crystal Growth and Design, 2017, 17, 5583-5585.	1.4	11
72	Molden 2.0: quantum chemistry meets proteins. Journal of Computer-Aided Molecular Design, 2017, 31, 789-800.	1.3	107

#	Article	IF	CITATIONS
73	Metal ion-exchange on the muscovite mica surface. Surface Science, 2017, 665, 56-61.	0.8	28
74	Polymorphism and Modulation of Para-Substituted l-Phenylalanine. Crystal Growth and Design, 2017, 17, 6231-6238.	1.4	1
75	Deracemization of a Racemic Allylic Sulfoxide Using Viedma Ripening. Crystal Growth and Design, 2017, 17, 4454-4457.	1.4	25
76	Flexible shielding layers for solar cells in space applications. Journal of Applied Polymer Science, 2016, 133, .	1.3	21
77	Solid–Liquid Interface Structure of Muscovite Mica in CsCl and RbBr Solutions. Langmuir, 2016, 32, 12955-12965.	1.6	38
78	Degradation mechanism(s) of GaAs solar cells with Cu contacts. Physical Chemistry Chemical Physics, 2016, 18, 10232-10240.	1.3	11
79	Preparation of a smooth GaN–Gallium solid–liquid interface. Journal of Crystal Growth, 2016, 448, 70-75.	0.7	7
80	Solvates, Salts, and Cocrystals: A Proposal for a Feasible Classification System. Crystal Growth and Design, 2016, 16, 3237-3243.	1.4	191
81	Speeding up Viedma ripening. Chemical Communications, 2016, 52, 12048-12051.	2.2	19
82	Deracemization of a Racemic Compound via Its Conglomerate-Forming Salt Using Temperature Cycling. Crystal Growth and Design, 2016, 16, 5563-5570.	1.4	63
83	Resolution of asparagine in a coupled batch grinding process: experiments and modelling. CrystEngComm, 2016, 18, 9252-9259.	1.3	7
84	Persistent Reverse Enantiomeric Excess in Solution during Viedma Ripening. Crystal Growth and Design, 2016, 16, 4752-4758.	1.4	10
85	Impact of shading on a flat CPV system for façade integration. Solar Energy, 2016, 140, 162-170.	2.9	16
86	The role of surface and interface structure in crystal growth. Progress in Crystal Growth and Characterization of Materials, 2016, 62, 203-211.	1.8	5
87	Creeping: an efficient way to determine the anticaking ability of additives for sodium chloride. CrystEngComm, 2016, 18, 6176-6183.	1.3	13
88	Structure and activity of the anticaking agent iron( <scp>iii</scp> ) meso-tartrate. Dalton Transactions, 2016, 45, 6650-6659.	1.6	7
89	3,4-Dimethoxybenzaldehyde. IUCrData, 2016, 1, .	0.1	3
90	Understanding the polymorphic phase transitions of linear amino acids using in situ characterisation. Acta Crystallographica Section A: Foundations and Advances, 2016, 72, s67-s67.	0.0	0

#	Article	IF	CITATIONS
91	Oneâ€Pot Synthesis, Crystallization and Deracemization of Isoindolinones from Achiral Reactants. European Journal of Organic Chemistry, 2015, 2015, 7249-7252.	1.2	7
92	Linear Deracemization Kinetics during Viedma Ripening: Autocatalysis Overruled by Chiral Additives. Crystal Growth and Design, 2015, 15, 1975-1982.	1.4	33
93	A Comparative Study of Impurity Effects on Protein Crystallization: Diffusive versus Convective Crystal Growth and Design, 2015, 15, 1150-1159.	1.4	26
94	A practical kit for micro-scale application of the ceiling crystallisation method. CrystEngComm, 2015, 17, 2602-2605.	1.3	6
95	Viedma ripening: a reliable crystallisation method to reach single chirality. Chemical Society Reviews, 2015, 44, 6723-6732.	18.7	165
96	Sodium Chloride Dihydrate Crystals: Morphology, Nucleation, Growth, and Inhibition. Crystal Growth and Design, 2015, 15, 3166-3174.	1.4	20
97	Effects of copper diffusion in gallium arsenide solar cells for space applications. Solar Energy Materials and Solar Cells, 2015, 140, 45-53.	3.0	15
98	A sample chamber for in situ high-energy X-ray studies of crystal growth at deeply buried interfaces in harsh environments. Journal of Crystal Growth, 2015, 420, 84-89.	0.7	10
99	Influence of anticaking agents on the caking of sodium chloride at the powder and two-crystal scale. Powder Technology, 2015, 277, 262-267.	2.1	19
100	Versatile Wedge-Based System for the Construction of Unidirectional Collagen Scaffolds by Directional Freezing: Practical and Theoretical Considerations. ACS Applied Materials & Interfaces, 2015, 7, 8495-8505.	4.0	70
101	Polymer versus Monomer Action on the Growth and Habit Modification of Sodium Chloride Crystals. Crystal Growth and Design, 2015, 15, 5375-5381.	1.4	19
102	Deracemization Controlled by Reaction-Induced Nucleation: Viedma Ripening as a Safety Catch for Total Spontaneous Resolution. Crystal Growth and Design, 2015, 15, 3917-3921.	1.4	21
103	Emergence of single-molecular chirality from achiral reactants. Nature Communications, 2014, 5, 5543.	5.8	66
104	Atomic layering and misfit-induced densification at the Si(111)/In solid–liquid interface. Surface Science, 2014, 621, 69-76.	0.8	7
105	Formation of a Salt Enables Complete Deracemization of a Racemic Compound through Viedma Ripening. Crystal Growth and Design, 2014, 14, 1744-1748.	1.4	48
106	Muscovite mica: Flatter than a pancake. Surface Science, 2014, 619, 19-24.	0.8	61
107	Illuminating protein crystal growth using fluorophore-labelled proteins. CrystEngComm, 2014, 16, 9800-9809.	1.3	5
108	Dibenzo Crown Ether Layer Formation on Muscovite Mica. Langmuir, 2014, 30, 12570-12577.	1.6	9

#	Article	IF	CITATIONS
109	Theoretical review of series resistance determination methods for solar cells. Solar Energy Materials and Solar Cells, 2014, 130, 605-614.	3.0	27
110	Enantiopure Isoindolinones through Viedma Ripening. Chemistry - A European Journal, 2014, 20, 13527-13530.	1.7	37
111	Temperature-dependent structure, elasticity, and entropic stability of Bi phases on Cu{111}. Physical Review B, 2014, 89, .	1.1	4
112	Experimental review of series resistance determination methods for III–V concentrator solar cells. Solar Energy Materials and Solar Cells, 2014, 130, 364-374.	3.0	14
113	Integration techniques for surface X-ray diffraction data obtained with a two-dimensional detector. Journal of Applied Crystallography, 2014, 47, 365-377.	1.9	38
114	Symmetry and symmetry breaking during crystal growth. Acta Crystallographica Section A: Foundations and Advances, 2014, 70, C940-C940.	0.0	0
115	Controlling the Effect of Chiral Impurities on Viedma Ripening. Crystal Growth and Design, 2013, 13, 4776-4780.	1.4	36
116	Complexity from Simplicity. Science, 2013, 340, 822-823.	6.0	6
117	High Resolution Protein Crystals Using an Efficient Convection-Free Geometry. Crystal Growth and Design, 2013, 13, 775-781.	1.4	19
118	Space environmental testing of flexible coverglass alternatives based on siloxanes. Polymer Degradation and Stability, 2013, 98, 2503-2511.	2.7	14
119	The development of the depletion zone during ceiling crystallization: phase shifting interferometry and simulation results. CrystEngComm, 2013, 15, 2275.	1.3	12
120	Arsenic Formation on GaAs during Etching in HF Solutions: Relevance for the Epitaxial Lift-Off Process. ECS Journal of Solid State Science and Technology, 2013, 2, P58-P65.	0.9	36
121	Record resolution protein crystals using an efficient convection-free growth geometry. Acta Crystallographica Section A: Foundations and Advances, 2012, 68, s10-s10.	0.3	0
122	Phase Transition Driven Discontinuity in Thermodynamic Size Selection. Physical Review Letters, 2012, 109, 195501.	2.9	5
123	Anticaking Activity of Ferrocyanide on Sodium Chloride Explained by Charge Mismatch. Crystal Growth and Design, 2012, 12, 1919-1924.	1.4	44
124	Structure of singly terminated polar DyScO <mml:math xmlns:mml="http://www.w3.org/1998/Math/MathML" display="inline"&gt;<mml:msub><mml:mrow /&gt;<mml:mn>3</mml:mn></mml:mrow </mml:msub>(110) surfaces. Physical Review B, 2012, 85, .</mml:math 	1.1	17
125	Anomalous IV-characteristics of a GaAs solar cell under high irradiance. Solar Energy Materials and Solar Cells, 2012, 104, 97-101.	3.0	10
126	Monolayer and aggregate formation of a modified phthalocyanine on mica determined by a delicate balance of surface interactions. Surface Science, 2012, 606, 830-835.	0.8	10

#	Article	IF	CITATIONS
127	Surface Degradation during Separation of Crystals from Solution: Minimizing the Shut-off Effect. Crystal Growth and Design, 2012, 12, 2265-2271.	1.4	4
128	Complete Deracemization of Proteinogenic Glutamic Acid Using Viedma Ripening on a Metastable Conglomerate. Crystal Growth and Design, 2012, 12, 5796-5799.	1.4	51
129	Growth Inhibition of Sodium Chloride Crystals by Anticaking Agents: In Situ Observation of Step Pinning. Crystal Growth and Design, 2012, 12, 5889-5896.	1.4	21
130	Formation of Wurtzite InP Nanowires Explained by Liquid-Ordering. Nano Letters, 2011, 11, 44-48.	4.5	22
131	Crystal Structure Transfer in Core/Shell Nanowires. Nano Letters, 2011, 11, 1690-1694.	4.5	93
132	The Role of Surface Energies and Chemical Potential during Nanowire Growth. Nano Letters, 2011, 11, 1259-1264.	4.5	92
133	A genuine circular contact grid pattern for solar cells. Progress in Photovoltaics: Research and Applications, 2011, 19, 517-526.	4.4	12
134	X-ray diffraction analysis of the silicon (111) surface during alkaline etching. Surface Science, 2011, 605, 1027-1033.	0.8	4
135	Realising epitaxial growth of GaN on (001) diamond. Journal of Applied Physics, 2011, 110, .	1.1	22
136	IsoQuestCSP: analyzing sets of predicted crystal structures and selecting the true structure. Acta Crystallographica Section A: Foundations and Advances, 2011, 67, C33-C34.	0.3	0
137	Correlated Twins in Nanowires. Microscopy and Microanalysis, 2010, 16, 1808-1809.	0.2	0
138	Absolute etch rates in alkaline etching of silicon (111). Sensors and Actuators A: Physical, 2010, 164, 154-160.	2.0	12
139	Enantioselective Symmetry Breaking Directed by the Order of Process Steps. Angewandte Chemie - International Edition, 2010, 49, 2539-2541.	7.2	41
140	The Driving Mechanism Behind Attritionâ€Enhanced Deracemization. Angewandte Chemie - International Edition, 2010, 49, 8435-8438.	7.2	139
141	Enhanced growth rates and reduced parasitic deposition by the substitution of Cl2 for HCl in GaN HVPE. Journal of Crystal Growth, 2010, 312, 2542-2550.	0.7	7
142	The nucleation of HCl and Cl2-based HVPE GaN on mis-oriented sapphire substrates. Physica Status Solidi C: Current Topics in Solid State Physics, 2010, 7, 1749-1755.	0.8	0
143	Generic nano-imprint process for fabrication of nanowire arrays. Nanotechnology, 2010, 21, 065305.	1.3	70
144	A new circular contact grid pattern, designed for solar cells in a mechanical stack. , 2010, , .		0

#	Article	IF	CITATIONS
145	Comparison of GaN and AlN nucleation layers for the oriented growth of GaN on diamond substrates. Diamond and Related Materials, 2010, 19, 437-440.	1.8	16
146	Paired Twins and {112i} Morphology in GaP Nanowires. Nano Letters, 2010, 10, 2349-2356.	4.5	41
147	Self-Assembly of Porphyrins on a Single Crystalline Organic Substrate. Langmuir, 2010, 26, 498-503.	1.6	8
148	Scaling Up Attrition-Enhanced Deracemization by Use of an Industrial Bead Mill in a Route to Clopidogrel (Plavix). Organic Process Research and Development, 2010, 14, 908-911.	1.3	72
149	Crystal Morphology. , 2010, , .		0
150	Periodic nanowire structures. , 2010, , .		0
151	Efficient Havinga–Kondepudi resolution of conglomerate amino acid derivatives by slow cooling and abrasive grinding. CrystEngComm, 2010, 12, 2051.	1.3	20
152	Kinetic switching between two modes of bisurea surfactant self-assembly. Chemical Communications, 2010, 46, 6063.	2.2	16
153	Complete Chiral Resolution Using Additiveâ€Induced Crystal Size Bifurcation During Grinding. Angewandte Chemie - International Edition, 2009, 48, 3278-3280.	7.2	71
154	Fast Attritionâ€Enhanced Deracemization of Naproxen by a Gradual Inâ€Situ Feed. Angewandte Chemie - International Edition, 2009, 48, 4581-4583.	7.2	91
155	From Ostwald Ripening to Single Chirality. Angewandte Chemie - International Edition, 2009, 48, 9600-9606.	7.2	183
156	Growth of scandium aluminum nitride nanowires on ScN(111) films on 6H‣iC substrates by HVPE. Physica Status Solidi (A) Applications and Materials Science, 2009, 206, 2809-2815.	0.8	7
157	Complete chiral symmetry breaking of an amino acid derivative directed by circularly polarized light. Nature Chemistry, 2009, 1, 729-732.	6.6	210
158	The solubility behaviour and thermodynamic relations of the three forms of Venlafaxine free base. International Journal of Pharmaceutics, 2009, 368, 146-153.	2.6	19
159	Surface alloying and anomalous diffusion of Bi on Cu(111). Surface Science, 2009, 603, 3292-3296.	0.8	13
160	Wet chemical etching of silicon {111}: Etch pit analysis by the Lichtfigur method. Journal of Crystal Growth, 2009, 311, 1371-1377.	0.7	11
161	ScAlN nanowires: A cathodoluminescence study. Journal of Crystal Growth, 2009, 311, 3147-3151.	0.7	14
162	On the nucleation, coalescence, and overgrowth of HVPE GaN on misoriented sapphire substrates and the origin of pinholes. Journal of Crystal Growth, 2009, 311, 4685-4691.	0.7	13

#	Article	IF	CITATIONS
163	Study of the Needle-Like Morphologies of Two β-Phthalocyanines. Crystal Growth and Design, 2009, 9, 840-847.	1.4	24
164	Influence of Additives on Alkaline Etching of Silicon(111). Crystal Growth and Design, 2009, 9, 4315-4323.	1.4	10
165	Analysis of Growth Spirals on Vapor-Grown Metal-free β-Phthalocyanine Crystals. Crystal Growth and Design, 2009, 9, 2409-2414.	1.4	2
166	Simple Geometry for Diffusion Limited Protein Crystal Growth: Harnessing Gravity to Suppress Convection. Crystal Growth and Design, 2009, 9, 885-888.	1.4	15
167	Attrition-Enhanced Deracemization in the Synthesis of Clopidogrel - A Practical Application of a New Discovery. Organic Process Research and Development, 2009, 13, 1195-1198.	1.3	115
168	Growth of GaN on nano-crystalline diamond substrates. Diamond and Related Materials, 2009, 18, 1043-1047.	1.8	28
169	Hydration and Dehydration of the Pure Enantiomer and the Racemic of Phencyphos. , 2009, , .		0
170	Polymorph prediction of organic pigments. Dyes and Pigments, 2008, 79, 183-192.	2.0	15
171	Complete Deracemization by Attritionâ€Enhanced Ostwald Ripening Elucidated. Angewandte Chemie - International Edition, 2008, 47, 6445-6447.	7.2	106
172	Attrition‣nhanced Deracemization of an Amino Acid Derivative That Forms an Epitaxial Racemic Conglomerate. Angewandte Chemie - International Edition, 2008, 47, 7226-7229.	7.2	118
173	Experimental and computational morphology of three polymorphs of the free base of Venlafaxine: A comparison of morphology prediction methods. International Journal of Pharmaceutics, 2008, 353, 113-123.	2.6	11
174	Twinning superlattices in indium phosphide nanowires. Nature, 2008, 456, 369-372.	13.7	625
175	The Critical Rayleigh Number in Low Gravity Crystal Growth from Solution. Crystal Growth and Design, 2008, 8, 2194-2199.	1.4	9
176	Emergence of a Single Solid Chiral State from a Nearly Racemic Amino Acid Derivative. Journal of the American Chemical Society, 2008, 130, 1158-1159.	6.6	424
177	Polymorphism and Migratory Chiral Resolution of the Free Base of Venlafaxine. A Remarkable Topotactical Solid State Transition from a Racemate to a Racemic Conglomerate. Crystal Growth and Design, 2008, 8, 71-79.	1.4	26
178	Growth Inhibition of Protein Crystals: A Study of Lysozyme Polymorphs. Crystal Growth and Design, 2008, 8, 270-274.	1.4	30
179	Explanation for the Emergence of a Single Chiral Solid State during Attrition-Enhanced Ostwald Ripening: Survival of the Fittest. Crystal Growth and Design, 2008, 8, 1675-1681.	1.4	118
180	A Comparison between Simulations and Experiments for Microgravity Crystal Growth in Gradient Magnetic Fields. Crystal Growth and Design, 2008, 8, 2200-2204.	1.4	5

#	Article	IF	CITATIONS
181	Wet Chemical Etching of Silicon {111}: Autocatalysis in Pit Formation. Journal of the Electrochemical Society, 2008, 155, J79.	1.3	16
182	Crystal growth in a three-phase system: Diffusion and liquid-liquid phase separation in lysozyme crystal growth. Physical Review E, 2007, 76, 011604.	0.8	13
183	Magnetically controlled gravity for protein crystal growth. Applied Physics Letters, 2007, 90, .	1.5	47
184	Spherulitic Growth of Hen Egg-White Lysozyme Crystals. Journal of Physical Chemistry B, 2007, 111, 1567-1573.	1.2	42
185	Towards an atomic-scale understanding of crystal growth in solution. Faraday Discussions, 2007, 136, 57.	1.6	12
186	Three-Dimensional Morphology of GaPâ^'GaAs Nanowires Revealed by Transmission Electron Microscopy Tomography. Nano Letters, 2007, 7, 3051-3055.	4.5	87
187	Epitaxy of Organic Crystal Films:Â Phenanthrene on Potassium Acid Phthalate. Crystal Growth and Design, 2007, 7, 243-249.	1.4	22
188	On the Definition of a Monte Carlo Model for Binary Crystal Growth. Journal of Physical Chemistry B, 2007, 111, 782-791.	1.2	6
189	Toward Rational Design of Tailor-made Additives Using Growth Site Statistics. Crystal Growth and Design, 2007, 7, 778-786.	1.4	11
190	The Step Energy as a Habit Controlling Factor:  Application to the Morphology Prediction of Aspartame, Venlafaxine, and a Yellow Isoxazolone Dye. Crystal Growth and Design, 2007, 7, 1949-1957.	1.4	13
191	PEG-Induced Morphologically Unstable Growth of Tetragonal Hen Egg-White Lysozyme Crystals. Crystal Growth and Design, 2007, 7, 1999-2008.	1.4	4
192	Steps on Surfaces in Modeling Crystal Growth. Crystal Growth and Design, 2007, 7, 1936-1942.	1.4	9
193	Polymorph Formation Studied by 3D Nucleation Simulations. Application to a Yellow Isoxazolone Dye, Paracetamol, andl-Glutamic Acid. Journal of Physical Chemistry B, 2007, 111, 1523-1530.	1.2	23
194	X-ray Diffraction Studies of Crystal-Vapor and Crystal-Solution Interfaces. AIP Conference Proceedings, 2007, , .	0.3	0
195	Polymorphic behavior of a yellow isoxazolone dye. Dyes and Pigments, 2007, 72, 339-344.	2.0	38
196	Interlaced spiral growth and step splitting on a steroid crystal. Journal of Crystal Growth, 2007, 299, 322-329.	0.7	9
197	Crystal structure prediction of organic pigments: quinacridone as an example. Journal of Applied Crystallography, 2007, 40, 105-114.	1.9	29
198	Rough Growth Behavior of a Polar Steroid Crystal:  A Case of Polymorphic Self-Poisoning?. Crystal Growth and Design, 2006, 6, 1311-1317.	1.4	13

#	Article	IF	CITATIONS
199	Morphology and Surface Structure of Silver Carboxylates. Crystal Growth and Design, 2006, 6, 1027-1032.	1.4	16
200	Liquid Ordering at the KDP {100}-Solution Interface. Crystal Growth and Design, 2006, 6, 588-591.	1.4	16
201	Dutch Resolution:  Nucleation Inhibition in an Ephedrineâ^'Cyclic Phosphoric Acid System. Crystal Growth and Design, 2006, 6, 861-865.	1.4	13
202	Using Gradient Magnetic Fields to Suppress Convection during Crystal Growth. Crystal Growth and Design, 2006, 6, 2275-2280.	1.4	29
203	Models for the determination of kinetic phase diagrams and kinetic phase separation domains. Calphad: Computer Coupling of Phase Diagrams and Thermochemistry, 2006, 30, 216-224.	0.7	7
204	Crystal structure prediction of organic pigments. Acta Crystallographica Section A: Foundations and Advances, 2006, 62, s79-s79.	0.3	0
205	On the determination of step energies. Theoretical considerations and application to an anisotropic Kossel model. Journal of Applied Crystallography, 2006, 39, 563-570.	1.9	11
206	Epitaxial 2D nucleation of the stable polymorphic form of the steroid 7αMNa on the metastable form: Implications for Ostwald's rule of stages. International Journal of Pharmaceutics, 2006, 309, 16-24.	2.6	21
207	Birth-and-spread growth on the Kossel and a non-Kossel surface. Journal of Crystal Growth, 2006, 286, 188-196.	0.7	16
208	An Atomic Force Microscopy Study of the (001) Surface of Triclinic Hen Egg-White Lysozyme Crystals. Crystal Growth and Design, 2006, 6, 1206-1213.	1.4	15
209	Stability of the polar {111} NaCl crystal face. Journal of Chemical Physics, 2006, 124, 164706.	1.2	31
210	Observation of a Liquid Phase with an Orthorhombic Orientational Order. Physical Review Letters, 2006, 96, 056102.	2.9	17
211	Microgravity crystal growth in a magnet. Acta Crystallographica Section A: Foundations and Advances, 2006, 62, s10-s10.	0.3	0
212	Heterogeneous 2D nucleation of the stable polymorphic form on the metastable form. Journal of Crystal Growth, 2005, 275, e1727-e1731.	0.7	10
213	Alizarin crystals: An extreme case of solvent induced morphology change. Journal of Crystal Growth, 2005, 285, 168-177.	0.7	22
214	Quantum mechanics calculations on the diastereomeric salts of cyclic phosphoric acids with ephedrine. Computational and Theoretical Chemistry, 2005, 717, 205-214.	1.5	0
215	Surface alloys, overlayer and incommensurate structures of Bi on Cu(111). Surface Science, 2005, 575, 233-246.	0.8	47
216	Structure of the {111} NaCl crystal surface grown from solution in the presence of CdCl2. Surface Science, 2005, 599, 196-206.	0.8	23

#	Article	IF	CITATIONS
217	pH-dependent liquid order at the solid-solution interface ofKH2PO4crystals. Physical Review B, 2005, 72, .	1.1	16
218	Suppression of convection using gradient magnetic fields during crystal growth of NiSO4â^™6H2O. Applied Physics Letters, 2005, 87, 214105.	1.5	21
219	Experimental and Computational Growth Morphology of Two Polymorphs of a Yellow Isoxazolone Dye. Langmuir, 2005, 21, 3831-3837.	1.6	10
220	Epitaxial 2D Nucleation of Metastable Polymorphs:  A 2D Version of Ostwald's Rule of Stages. Crystal Growth and Design, 2005, 5, 975-981.	1.4	57
221	Interface crystallography of a growing interface: KDP{101} and {100}. Acta Crystallographica Section A: Foundations and Advances, 2005, 61, c62-c62.	0.3	0
222	Crystal growth and morphology prediction of two quinacridone polymorphs. Acta Crystallographica Section A: Foundations and Advances, 2005, 61, c444-c444.	0.3	0
223	Nonequilibrium free energy and kinetic roughening of steps on the Kossel(001) surface. Physical Review B, 2004, 69, .	1.1	22
224	Liquid ordering at the Brushite-{010}–water interface. Physical Review B, 2004, 69, .	1.1	44
225	Nucleation and growth of crystalline ribbons in diastereomeric ephedrine–cyclic phosphoric acid systems. Journal of Crystal Growth, 2004, 265, 604-615.	0.7	3
226	Kink incorporation and step propagation in a non-Kossel model. Surface Science, 2004, 571, 41-62.	0.8	18
227	Kinetic roughening of Kossel and non-Kossel steps. Surface Science, 2004, 569, 33-46.	0.8	12
228	Formamide adsorption and habit changes of alkali halide crystals grown from solutions. Journal of Crystal Growth, 2004, 263, 544-551.	0.7	39
229	Thickness-dependent ordering of water layers at the NaCl(100) surface. Journal of Chemical Physics, 2004, 120, 9720-9724.	1.2	45
230	Crystal Growth and Morphology:  New Developments in an Integrated Hartmanâ^'PerdokConnected NetRoughening Transition Theory, Supported by Computer Simulations. Crystal Growth and Design, 2004, 4, 905-913.	1.4	50
231	Epitaxial Nucleation and Growth of n-Alkane Crystals on Graphite (0001). Crystal Growth and Design, 2004, 4, 361-367.	1.4	26
232	Determination of the Molecular Arrangement Inside Cyanine Dye Aggregates by Magnetic Orientation. Journal of Physical Chemistry B, 2004, 108, 16386-16391.	1.2	17
233	Understanding the Effect of a Solvent on the Crystal Habit. Crystal Growth and Design, 2004, 4, 765-768.	1.4	122
234	Characterization of solid—liquid interfaces using X-ray diffraction. Nanostructure Science and Technology, 2004, , 31-55.	0.1	4

#	Article	IF	CITATIONS
235	Growth and characterization of cesium halides with cubic morphologies. Journal of Crystal Growth, 2003, 253, 472-480.	0.7	3
236	Growth and characteristics of the NaCl crystal surface grown from solution. Surface Science, 2003, 523, 307-315.	0.8	55
237	The effects of kink correlation and the Monte Carlo probability scheme on the step structure and velocity. Surface Science, 2003, 525, 1-12.	0.8	23
238	Surface structure of potassium dichromate (KBC) crystals. Surface Science, 2003, 526, 133-140.	0.8	9
239	Liquid Order at the Interface of KDP Crystals with Water: Evidence for Icelike Layers. Physical Review Letters, 2003, 90, 066103.	2.9	102
240	Melting behavior of the $\hat{l}^2$ -Pb/Ge(111) structure. Physical Review B, 2003, 67, .	1.1	5
241	New(3×3)R30°Phase of Pb on Ge(111) and Its Consequence for the Melting Transition. Physical Review Letters, 2003, 90, 056104.	2.9	11
242	Submicron liquid crystal pixels on a nanopatterned indium tin oxide surface. Applied Physics Letters, 2002, 80, 4635-4637.	1.5	22
243	The structure of surface alloy phases on metallic substrates. Chemical Physics of Solid Surfaces, 2002, 10, 277-304.	0.3	9
244	Metastable States in Multicomponent Liquidâ^'Solid Systems II:  Kinetic Phase Separation. Journal of Physical Chemistry B, 2002, 106, 7331-7339.	1.2	18
245	Metastable States in Multicomponent Liquidâ^'Solid Systems I:  A Kinetic Crystallization Model. Journal of Physical Chemistry B, 2002, 106, 7321-7330.	1.2	23
246	In Situ Observation of Epitaxial Polymorphic Nucleation of the Model Steroid Methyl Analogue 17 Norethindrone. Journal of Physical Chemistry B, 2002, 106, 4725-4731.	1.2	34
247	Understanding crystal growth in vacuum and beyond. Surface Science, 2002, 500, 458-474.	0.8	39
248	Kink density and propagation velocity of the [] step on the Kossel () surface. Surface Science, 2002, 506, 183-195.	0.8	33
249	On the irrelevance of electrostatics for the crystal structures and polymorphism of long evenn-alkanes. Journal of Computational Chemistry, 2002, 23, 365-370.	1.5	6
250	On the influence of thermal motion on the crystal structures and polymorphism of even n-alkanes. Acta Crystallographica Section B: Structural Science, 2002, 58, 677-683.	1.8	7
251	Structure determination of Cu()–O using X-ray diffraction and DFT calculations. Surface Science, 2002, 516, 16-32.	0.8	25
252	Equilibrium morphologies and thermal roughening of cesium halides. Journal of Crystal Growth, 2002, 245, 171-179.	0.7	7

#	Article	IF	CITATIONS
253	On the influence of thermal motion on the crystal structures and polymorphism of even n-alkanes. Acta Crystallographica Section A: Foundations and Advances, 2002, 58, c51-c51.	0.3	1
254	In-situdetermination of polymorphic phase diagrams. Acta Crystallographica Section A: Foundations and Advances, 2002, 58, c144-c144.	0.3	0
255	Formation and stabilization of pyramidal etch hillocks on silicon {100} in anisotropic etchants: Experiments and Monte Carlo simulation. Journal of Applied Physics, 2001, 89, 4113-4123.	1.1	60
256	Compression versus expansion on ionic crystal surfaces. Physical Review B, 2001, 64, .	1.1	6
257	Oxidative etching of cleaved synthetic diamond {111} surfaces. Surface Science, 2001, 492, 91-105.	0.8	59
258	A Monte Carlo study of etching in the presence of a mask junction. Journal of Micromechanics and Microengineering, 2001, 11, 409-415.	1.5	8
259	Controlling Crystal Surface Termination by Cleavage Direction. Physical Review Letters, 2001, 86, 5070-5072.	2.9	14
260	Structure of liquid Sn on Ge(111). Physical Review B, 2001, 64, .	1.1	23
261	Atomic structure of diamond {111} surfaces etched in oxygen water vapor. Physical Review B, 2001, 64, .	1.1	33
262	Surface X-ray diffraction studies of crystal growth. , 2001, , 351-360.		1
263	Etching and surface termination of K2Cr2O7 {0 0 1} faces observed using in situ atomic force microscopy. Journal of Crystal Growth, 2000, 216, 413-427.	0.7	22
264	A Monte Carlo study of dislocation growth and etching of crystals. Journal of Crystal Growth, 2000, 219, 165-175.	0.7	23
265	ROD: a program for surface X-ray crystallography. Journal of Applied Crystallography, 2000, 33, 401-405.	1.9	316
266	Monte Carlo study of kinetic smoothing during dissolution and etching of the Kossel (100) and silicon (111) surfaces. Journal of Applied Physics, 2000, 88, 4595.	1.1	13
267	Phase transition of a Pb monolayer on Ge(111). Physical Review B, 1999, 59, 13301-13308.	1.1	27
268	X-ray diffraction studies of potassium dihydrogen phosphate (KDP) crystal surfaces. Journal of Crystal Growth, 1999, 205, 202-214.	0.7	75
269	Surface Atomic Structure of KDP Crystals in Aqueous Solution: An Explanation of the Growth Shape. Physical Review Letters, 1998, 80, 2229-2232.	2.9	140
270	A (2+3)-Type Surface Diffractometer: Mergence of the z-Axis and (2+2)-Type Geometries. Journal of Applied Crystallography, 1998, 31, 198-203.	1.9	90

#	Article	IF	CITATIONS
271	The Dutch–Belgian beamline at the ESRF. Journal of Synchrotron Radiation, 1998, 5, 518-520.	1.0	139
272	Evidence for tilted chains on the diamond (111)-(2 × 1) surface. Surface Science, 1998, 396, 241-252.	0.8	23
273	Surface atomic structure of the reconstructions of Ag(111) and Cu(111). Surface Science, 1998, 414, 159-169.	0.8	49
274	Floating Stacking Fault during Homoepitaxial Growth of Ag(111). Physical Review Letters, 1998, 81, 381-384.	2.9	15
275	Sb-enhanced nucleation in the homoepitaxial growth of Ag(111). Physical Review B, 1998, 57, 4127-4131.	1.1	68
276	Structure and morphology of the as-polished diamond(111)-1 × 1 surface. Surface Science, 1997, 387, 342-353.	0.8	24
277	A curved Micro-Strip Gas Counter for synchrotron radiation time resolved SAXS/WAXS experiments. Nuclear Instruments and Methods in Physics Research, Section A: Accelerators, Spectrometers, Detectors and Associated Equipment, 1997, 392, 83-88.	0.7	18
278	Integrated Intensities Using a Six-Circle Surface X-ray Diffractometer. Journal of Applied Crystallography, 1997, 30, 532-543.	1.9	288
279	Slits as Adjustable Pinholes for Coherent X-ray Scattering Experiments. Journal of Synchrotron Radiation, 1997, 4, 210-213.	1.0	13
280	Interface structure of Si(111)-(â^š3 × â^š3)R30º-ErSi2 â^' x. Surface Science, 1996, 345, 247-260.	0.8	35
281	Reversible place-exchange during film growth: a mechanism for surfactant transport. Surface Science, 1996, 355, L375-L380.	0.8	34
282	Surfactants used in Ag(111) homoepitaxy: Sb, In, Pt and O2. Surface Science, 1996, 365, 205-211.	0.8	12
283	Atomic structure and thermal stability of two-dimensional Er silicide on Si(111). Physical Review B, 1996, 54, 2004-2009.	1.1	40
284	An outâ€ofâ€plane detector for surface xâ€ray diffraction. Review of Scientific Instruments, 1996, 67, 2658-2659.	0.6	13
285	Incorporation and optical activation of erbium in silicon using molecular beam epitaxy. Journal of Applied Physics, 1996, 79, 2658-2662.	1.1	42
286	Surface X-ray crystallography of growing crystals and interfaces. Nuclear Instruments & Methods in Physics Research B, 1995, 97, 358-363.	0.6	4
287	Indium-induced lowering of the Schwoebel barrier in the homoepitaxial growth of Cu(100). Physical Review B, 1995, 51, 14806-14809.	1.1	57
288	Segregation and trapping of erbium during silicon molecular beam epitaxy. Applied Physics Letters, 1995, 66, 1385-1387.	1.5	47

#	Article	IF	CITATIONS
289	Importance of the additional step-edge barrier in determining film morphology during epitaxial growth. Physical Review B, 1995, 51, 14790-14793.	1.1	86
290	Thermal diffuse scattering from surface-melted Pb(110). Physical Review B, 1995, 51, 14753-14755.	1.1	4
291	A solution of the doping problem for Ga deltaâ€doping layers in Si. Journal of Applied Physics, 1995, 78, 4933-4938.	1.1	5
292	Indium-induced layer-by-layer growth and suppression of twin formation in the homoepitaxial growth of Cu(111). Physical Review B, 1995, 52, 17443-17448.	1.1	70
293	A study on the Si(111)-â^š3 × â^š3-Ag system II. Interaction between substrate and adsorbate. Surface Science, 1995, 330, 113-125.	0.8	14
294	The effect of Sb on the nucleation and growth of Ag on Ag(100). Surface Science, 1995, 330, 101-112.	0.8	33
295	Surfactant-Induced Layer-by-Layer Growth of Ag on Ag(111): Origins and Side Effects. Physical Review Letters, 1994, 72, 3843-3846.	2.9	284
296	Interface roughness during thermal and ionâ€induced regrowth of amorphous layers on Si(001). Applied Physics Letters, 1994, 64, 1803-1805.	1.5	22
297	The growth and atomic structure of the Si(1 1 1)-indium interface studied by surface X-ray diffraction. Physica B: Condensed Matter, 1994, 198, 246-248.	1.3	22
298	A study on the system. Surface Science, 1994, 304, 12-23.	0.8	12
299	Transient diffusion of Ga in amorphous silicon. Journal of Applied Physics, 1994, 76, 5719-5723.	1.1	12
300	Atomic Structure of Ultrathin Erbium Silicides on Si(111). Materials Research Society Symposia Proceedings, 1994, 355, 281.	0.1	2
301	Formation of ironsilicide on Si(001). Applied Surface Science, 1993, 70-71, 564-568.	3.1	1
302	Angle calculations for a six-circle surface X-ray diffractometer. Journal of Applied Crystallography, 1993, 26, 706-716.	1.9	92
303	Structure determination of the NiSi2(111) surface with medium-energy ion backscattering from individual monolayers. Surface Science, 1993, 290, 255-266.	0.8	10
304	Formation of epitaxial βâ€FeSi2films on Si(001) as studied by mediumâ€energy ion scattering. Journal of Applied Physics, 1993, 73, 1104-1109.	1.1	44
305	Structure of Ge(111)â^š3 × â^š3R30°-Au determined by surface x-ray diffraction. Physical Review B, 1993, 48, 1632-1642.	1.1	41
306	CoSi2/Si(111) interface: Determination of the interfacial metal coordination number. Physical Review B, 1992, 45, 6700-6708.	1.1	18

#	Article	IF	CITATIONS
307	Surfactant-induced layer-by-layer growth of Ag on Ag(111). Physical Review Letters, 1992, 68, 3335-3338.	2.9	400
308	Healing kinetics of a sputter-roughened surface. Surface Science, 1992, 261, 118-122.	0.8	5
309	X-ray reflectivity study of the Si(111)7 × 7 surface. Surface Science, 1992, 261, 123-128.	0.8	46
310	The growth of indium on the Si(111) surface studied by X-ray reflectivity and Auger electron spectroscopy. Surface Science, 1992, 277, 330-336.	0.8	46
311	Asymmetrical dimers on the Ge(001)-2 × 1-Sb surface observed using X-ray diffraction. Surface Science, 1992, 275, 190-200.	0.8	37
312	Epitaxial submonolayer cobalt films on Cu(100) studied by X-ray diffraction. Surface Science, 1991, 250, L363-L367.	0.8	16
313	Surface morphology of Ag(110) close to its roughening transition. Physical Review Letters, 1991, 67, 1890-1893.	2.9	54
314	X-ray Scattering from Interfaces. Materials Research Society Symposia Proceedings, 1991, 237, 359.	0.1	0
315	Epitaxial submonolayer cobalt films on Cu(100) studied by X-ray diffraction. Surface Science Letters, 1991, 250, L363-L367.	0.1	2
316	Structure analysis of Si(111)-(â^š3 × â^š3 )R30°/Ag using x-ray standing waves. Physical Review B, 1991, 43, 7185-7193.	1.1	89
317	X-Ray Diffraction From Surfaces and Interfaces: Atomic Structure and Morphology. Materials Research Society Symposia Proceedings, 1990, 202, 291.	0.1	0
318	X-ray Diffraction from Surfaces and Interfaces:Atomic Structure and Morphology. Materials Research Society Symposia Proceedings, 1990, 208, 169.	0.1	0
319	X-ray scattering studies of semiconductor interfaces: Atomic structure and morphology. Applied Surface Science, 1990, 41-42, 62-69.	3.1	3
320	The high temperature phase transition of Pt(110) (1 × 2). Vacuum, 1990, 41, 318-320.	1.6	6
321	Oxygen-induced missing-row reconstruction of Cu(001) and Cu(001)-vicinal surfaces. Physical Review B, 1990, 42, 6954-6962.	1.1	105
322	Robinson, Vlieg, and Kern reply. Physical Review Letters, 1990, 65, 1831-1831.	2.9	8
323	Grazing-incidence x-ray study of the charge-density-wave phase transition inK0.3MoO3. Physical Review B, 1990, 42, 8791-8794.	1.1	10
324	Surface-induced heterophase fluctuation. Physical Review Letters, 1990, 65, 2692-2695.	2.9	14

#	Article	IF	CITATIONS
325	Structure determination of Cu(100)-p(2×2)-S using x-ray diffraction. Physical Review B, 1990, 41, 7896-7898.	1.1	32
326	Structure and roughening of the Pt(110) surface. Faraday Discussions of the Chemical Society, 1990, 89, 159.	2.2	5
327	Relaxations in the missing-row structure of the (1 × 2) reconstructed surfaces of Au(110) and Pt(110). Surface Science, 1990, 233, 248-254.	0.8	136
328	Non-Ising behavior of the Pt(110) surface phase transition. Physical Review Letters, 1989, 63, 2578-2581.	2.9	134
329	Structure determination of the Si(111):B(â^š3×â^š3)R30° surface: Subsurface substitutional doping. Physical Review Letters, 1989, 63, 1253-1256.	2.9	204
330	X-ray scattering from a vicinal Ge(001) surface. Journal of Physics Condensed Matter, 1989, 1, SB275-SB277.	0.7	3
331	The structure of Si(111)-()R30°-Ag determined by surface X-ray diffraction. Surface Science, 1989, 209, 100-114.	0.8	104
332	The structure of the surface determined using X-ray diffraction. Surface Science, 1989, 215, 555-565.	0.8	53
333	X-ray diffraction from rough, relaxed and reconstructed surfaces. Surface Science, 1989, 210, 301-321.	0.8	133
334	Surface X-Ray Scattering during Crystal Growth: Ge on Ge(111). Physical Review Letters, 1988, 61, 2241-2244.	2.9	155
335	Structure determination of theCoSi2:Si(111) interface by x-ray standing-wave analysis. Physical Review B, 1987, 36, 4769-4773.	1.1	101
336	An ultrahigh-vacuum chamber for surface X-ray diffraction combined with MBE. Nuclear Instruments and Methods in Physics Research, Section A: Accelerators, Spectrometers, Detectors and Associated Equipment, 1987, 262, 522-527.	0.7	68
337	Angle calculations for a five-circle diffractometer used for surface X-ray diffraction. Journal of Applied Crystallography, 1987, 20, 330-337.	1.9	48
338	Geometric structure of the NiSi2î—,Si(111) interface: An X-ray standing-wave analysis. Surface Science, 1986, 178, 36-46.	0.8	133
339	The superionic phase transition of fluorite-type crystals. Journal of Physics and Chemistry of Solids, 1986, 47, 521-528.	1.9	15
340	(n,l)â^'Subshell electron capture cross sections in collisions of C4+, N5+ and O6+ with atomic hydrogen. Nuclear Instruments & Methods in Physics Research B, 1985, 9, 403-407.	0.6	4
341	Subshell-selective electron capture cross sections in collisions of He2+and C4+with atomic hydrogen. Journal of Physics B: Atomic and Molecular Physics, 1985, 18, L17-L22.	1.6	19
342	Selective electron capture into He II (n, l) subshells in collisions of He2+with atomic and molecular hydrogen. Journal of Physics B: Atomic and Molecular Physics, 1985, 18, 4745-4762.	1.6	53